ECS Journal of Solid State Science and Technology, **5** (9) Q219-Q221 (2016)

Communication—Hourglass-Shaped Metal-Filament Switching Device with Multi-Layer (AlO_X/TiO_2) Oxide Electrolytes

Seokjae Lim, Jiyong Woo, Sangheon Lee, Jaesung Park, and Hyunsang Hwang[z]

Department of Materials Science and Engineering, Pohang University of Science and Technology, Pohang 790-784, Korea

This paper proposes using hourglass-shaped metal filaments to improve the ON/OFF resistance ratio and retention characteristics of switching devices used in reconfigurable logic applications. These filaments are obtained by controlling the Cu-ion mobility in multi-layer oxide electrolytes. By adopting an upper AlO_X and lower TiO_2 electrolyte layers with respectively low and high Cu-ion mobility, we could form hourglass-shaped filaments as a result of suppressed Cu-ion injection and enhanced filament lateral growth. The hourglass-shaped metal filaments induced local Joule heating at the filament constriction, thus accelerating RESET operations. We confirmed that, as a result, $Cu/AlO_X/TiO_2/W$ devices show high ON/OFF resistance ratios ($>10^6$) and ~10-year retention properties at 80°C.

[DOI: 10.1149/2.0031609jss]

Manuscript submitted April 11, 2016; revised manuscript received June 9, 2016. Published July 8, 2016.

Programmable metallization cells (PMCs) are one of the promising types of switching devices for use in reconfigurable field programmable gate arrays (FPGAs), because of their scaling potential, low power consumption, high ON/OFF resistance ratio, etc.[1–4]

The switching mechanism of PMCs can be explained by the formation and rupture of active metal (Ag or Cu) filaments in insulating solid electrolytes.[1] Conductive filament formation (dissolution) occurs under positive (negative) electric potentials at the active electrode, and is referred to as the SET (RESET) process. With the SET and RESET processes, devices enter the low resistance state (LRS) and high resistance state (HRS), respectively.

Even though PMC devices with chalcogenide materials show high ON/OFF resistance ratios adequate for FPGA applications, they exhibit poor retention properties and low glass transition temperatures.[4–10]

In this paper, we propose a PMC device with multi-layer oxide electrolytes for FPGA applications. We use a 3-nm-thick Al_2O_3 layer, because of the large band-gap and low ionic mobility of Cu.[11] Furthermore, an additional TiO_2 layer serves to introduce an element with high ionic mobility of Cu, thus allowing the optimum control of Cu diffusion and the formation of hourglass-shaped (HG) filaments. As a result, both high ON/OFF resistance ratios and good data retention capabilities are achieved.

Experimental

The PMC devices were fabricated on 300-nm-diameter W bottom electrodes. The 300-nm-diameter spacer was patterned by E-beam lithography through 90-nm-thick SiO_2. After spacer patterning, W-deposition was performed using physical vapor deposition, and the electrodes were made by chemical mechanical polishing. Next, 3-nm-thick Al_2O_3 and 1-nm-thick TiO_2 layers were deposited by atomic layer deposition (ALD) using trimethylaluminum, tetraisopropoxide, and H_2O precursors. Having completed that, 50-nm-thick Cu electrodes were deposited by DC sputtering from a Cu target. Finally, oxygen-deficient AlO_X was formed by a controlled H_2O pulse during ALD. The fabricated PMC devices were electrically tested using an Agilent B1500A semiconductor device analyzer.

Results and Discussion

Fig. 1a compares the Cu-ion mobility in the different oxide electrolytes from the physical tunneling gap reduction induced by Cu thermal diffusion.[3] The fast Cu-ion mobility in TiO_2 was confirmed by the steep decrease in resistance observed after thermal annealing. In addition, the lower forming voltage (the first SET) of the TiO_2 electrolyte (see Fig. 1b) supports the notion of a higher Cu-ion mobility in the TiO_2.[12] Fig. 1c shows the $Cu/Al_2O_3/TiO_2/W$ PMC device structure. The HG filament formation was expected, because of the adoption of a multi-layer oxide structure consisting of both high and low Cu-ion mobility materials.[13,14] Although the HG-filament PMC was expected to show high uniformity, fast switching, and excellent memory disturb characteristics, insufficient ON/OFF resistance ratios were observed, which might be attributed to the persistence of partial Cu-filaments after the RESET process.[15,16]

Consequently, we adopted oxygen-deficient AlO_X as an upper oxide, to suppress the formation of bulky upper HG filaments and accelerate filament rupture during the RESET process. We also obtained switching behaviors with high ON/OFF resistance ratios in the multi-layer and defect-engineered oxide-electrolyte-based PMC devices (AlO_X/TiO_2), as shown in Fig. 2a. The AlO_X/TiO_2-based PMC

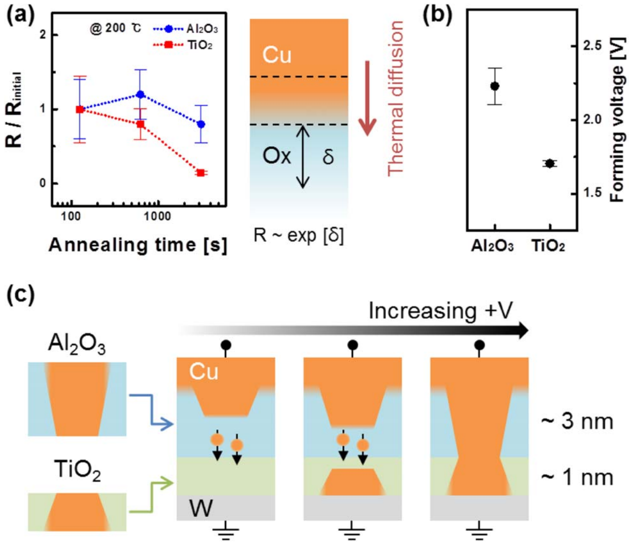

Figure 1. (a) Changes in the resistance of the Cu/Oxide/W structure caused by Cu thermal diffusion at 200°C. (b) Forming voltages for Al_2O_3 and TiO_2 PMCs with a Cu/Oxide/W structure. The oxide thickness in both (a) and (b) was ~3 nm. (c) Expected HG Cu-filament formation by the high and low Cu-ion mobility multi-layer oxide structure.

---

[z] E-mail: hwanghs@postech.ac.kr

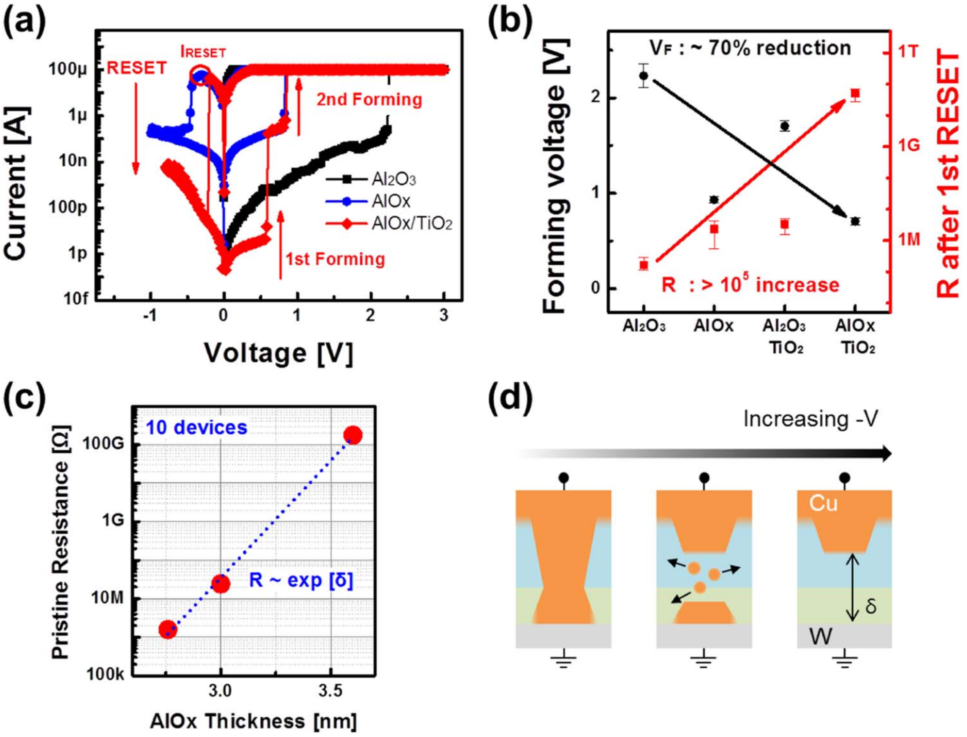

Figure 2. (a) Typical DC I-V curves for the Al_2O_3, AlO_X, and AlO_X/TiO_2 electrolyte-based PMC devices. High forming voltages and two-step forming can be seen for the Al_2O_3- and AlO_X/TiO_2-based PMC devices, respectively. (b) Forming voltage and resistance after the first RESET process, for various PMC structures. (c) Pristine resistance for various AlO_X thicknesses. (d) Schematic diagram of the RESET process of the fabricated AlO_X/TiO_2-based PMC device.

exhibited a two-step forming curve. The I-V trace (red-line) of the AlO_X/TiO_2 PMC followed that of the AlO_X PMC (blue-line) after the first forming. This means that the first and second forming steps were attributable to the TiO_2 and AlO_X breakdown, respectively, as depicted in Fig. 1c. The distributions of the forming voltage and HRS resistance after the first RESET for various PMC structures are plotted in Fig. 2b. The optimum 3-nm AlO_X/1-nm TiO_2 multi-layer PMC structure exhibited the highest HRS resistance with high ON/OFF resistance ratio. In addition, the devices with lower forming voltages exhibited higher HRS resistances, which were related to the Cu-filament size. In other words, larger Cu-filaments—which are harder to fully remove during the RESET process—would be formed by larger forming voltages.[17] The electron tunneling gap after the RESET process could be estimated by the pristine resistance of the insulator (Fig. 2c).[3] From Figs. 2b and 2c, we conclude that the tunneling gap after the RESET process became larger than 3.5 nm, a value similar to the thickness of the deposited oxide (see Fig. 2d). This full dissolution of the filament during the RESET process can be explained by the enhanced Cu back diffusion resulting from the localized Joule heating at the constriction part of the HG filament, and the high Cu-ion mobility in the TiO_2 layer.[18,19]

The upper part of the HG filament behaves as a Cu-ion supplying layer, but with a confined area when compared to the bulk Cu electrode. The lower part of the HG filament acts as a lightning rod, leading to the Cu-filament establishment.[20,21] When the upper part of the HG filament becomes bulky, a large Cu-ion supply area will be formed, resulting in an uncontrollably large Cu-filament. As shown in Figs. 3a and 3c, even though the thickness of Al_2O_3 was reduced, a large forming voltage and bulk filament formation were observed without sufficient defective sites in the Al_2O_3. When the thickness of TiO_2 was increased to obtain a larger pristine tunneling gap, we also observed the appearance of a high forming voltage and RESET current, as shown in Fig. 3b. The high forming voltage can be attributed to electric field relaxation, which resulted in a large conductive filament (see Fig. 3c). Therefore, we concluded that the multi-layer PMC composed of a defective upper AlO_X and thin TiO_2 showed the best ON/OFF resistance ratio, as a result of its optimum HG filament formation.

The ON/OFF resistance distribution was obtained from fabricated Cu/AlO_X/TiO_2/W devices, and is shown in Fig. 4a. A high ON/OFF resistance ratio ($>10^6$) was obtained between the median resistance

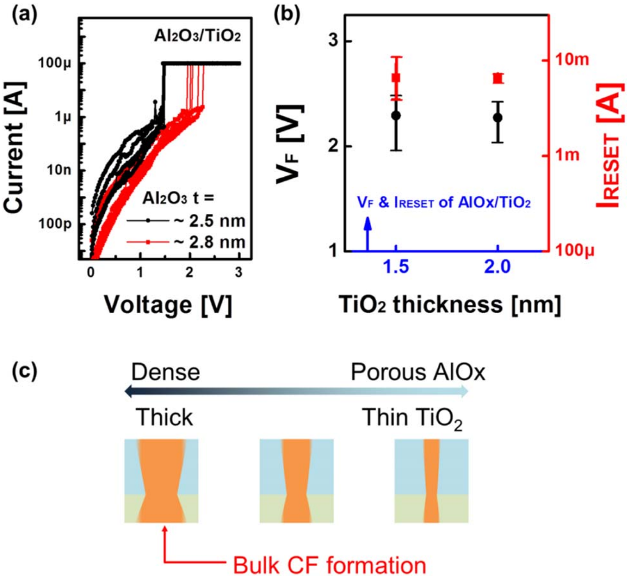

Figure 3. (a), (b) High forming voltage and RESET current were observed for the stoichiometric Al_2O_3-based, Al_2O_3/TiO_2, and thick TiO_2-based AlO_X/TiO_2 PMCs. (c) Bulky conductive filament formation phenomena resulting from the suppressed Cu migration through the upper oxide region, and the increased forming voltage.

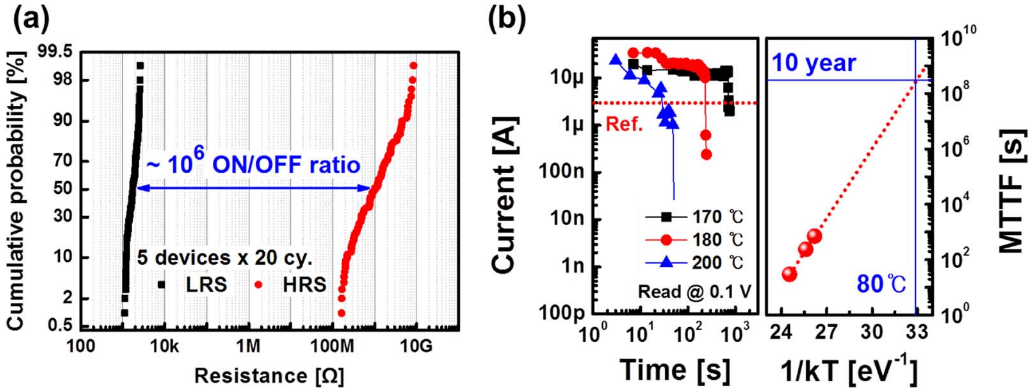

Figure 4. (a) ON/OFF resistance ratio distribution obtained from five different devices. An ON/OFF resistance ratio greater than 10^6 was confirmed on the median resistance values. (b) LRS retention characteristics and expected retention time at 80°C, according to the MTTF data for different temperatures.

values, a value that is suitable for reconfigurable FPGA applications.[12] Furthermore, we confirmed the retention characteristics of ∼10 years at 80°C through mean time to failure (MTTF) measurements based on the temperature-accelerated retention test; this is shown in Fig. 4b.

Summary

In this work, we explored the effects of the oxide electrolyte Cu-ion mobility on the Cu filament shape. In particular, we successfully created HG filaments by using a multi-oxide structure consisting of layers with different Cu-ion mobilities. In addition, engineering defects in the upper oxide electrolyte resulted in the creation of optimum conditions for the formation of HG Cu filaments. As a result, Cu/AlO_X/TiO_2/W devices exhibited the high ON/OFF resistance ratios and strong data retention properties necessary to produce PMCs for reconfigurable FPGA applications.

Acknowledgments

This work was supported by the Future Semiconductor Device Technology Development Program (10045085) funded By MOTIE (Ministry of Trade, Industry & Energy) and KSRC (Korea Semiconductor Research Consortium).

References

1. R. Waser, R. Dittmann, G. Staikov et al., *Adv. Mater.*, **21**, 2632 (2009).
2. R. Soni, M. Meier, A. Rüdiger et al., *Microelectronic Engineering*, **86**, 1054 (2009).
3. L. Goux, K. Sankaran, G. Kar et al., VLSI Technol., Dig. Tech. Pap. 69 (2012).
4. E. Vianello, O. Thomas, G. Molas et al., IEDM Tech. Dig. 6.3.1-6.3.4 (2014).
5. E. Vianello, G. Molas, F. Longnos et al., IEDM Tech. Dig. 31.5.1-31.5.4 (2012).
6. M. Mitkova, Y. Wang, and P. Boolchand, *Phys. Rev. Lett.*, **83**, 3848 (1999).
7. M. Saremi, *Solid State Ionics*, **290**, 1 (2016).
8. M. Saremi, H. J. Barnaby, A. Edwards et al., *ECS Electrochemistry Letters*, **4**(7), H29 (2015).
9. S. Rajabi, M Saremi, H. J. Barnaby et al., *Solid State Electronics*, **106**, 27 (2015).
10. M. Saremi, S. Rajabi, H. J. Barnaby et al., *MRS Proceedings*, **1692** (2014).
11. S. Lim, S. Lee, J. Woo et al., *ECS Solid State Lett.*, **4**(7) (2015).
12. T. Sakamoto, N Banno, N. Iguchi et al., VLSI Technol., *Dig. Tech. Pap.* 38 (2007).
13. Y. Yang, P. Gao, L. Li et al., *Nat. Commun.*, **5**, 4232 (2014).
14. J. Woo, A. Belmonte, A. Redolfi et al., *Journal of the Electron Devices Society*, **4**(3), 163 (2016).
15. A. Belmonte, U. Celano, A. Redolfi et al., *Transactions on Electron Devices*, **62**(6), 2007 (2015).
16. U. Celano, L. Goux, A. Belmonte et al., IEDM Tech. Dig. 14.1.1-14.1.4 (2014).
17. J. Guy, G. Molas, P. Blaise et al., IEDM Tech. Dig. 6.5.1-6.5.4 (2014).
18. T. Sakamoto, M. Tada, N. Banno et al., VLSI Technol., Dig. Tech. Pap. 130 (2009).
19. U. Russo, D. Ielmini, C. Cagli et al., IEDM Tech. Dig. 775 (2007).
20. S. Yu, X. Guan, and H.-S. P. Wong, IEDM Tech. Dig. 17.3.1-17.3.4 (2011).
21. D. Lee, J. Song, J. Woo et al., *Electron Device Lett.*, **35**(2), 214 (2014).